Numerical simulation of the spreading of aerated and nonaerated turbulent water jet in a tank with finite water depth

Yakun Guo[1]

Abstract: Numerical simulations are carried out to investigate the spreading of two-dimensional plane turbulent aerated and nonaerated jets in a tank filled with finite water depth. A multiphase model is applied to simulate the problem under investigation. The governing equations, their numerical scheme and the boundary conditions are presented. Aerated and non-aerated turbulent jets are simulated for a range of the jet velocity and width at exit, the initial air content at exit and the water depth in tank. The simulated results show that a self-similar Gaussian velocity distribution exists from the distance downstream being larger than five jet slot width for both the aerated and nonaerated jets. Good agreement between the simulated velocity profiles and available laboratory experiments is obtained. The simulated slope of the jet velocity decay along the jet centreline is in good agreement with the experimental measurements. The effect of air content on pressure distribution and the maximum impinging hydrodynamic pressure at the tank bottom is discussed.

Key words: numerical simulation; turbulence; jet; air content

Introduction

Plunge pool scour generated by free trajectory jets is one of key problems in the design and operation of a hydro scheme. The development of plunge pool scour can

[1]Reader, School of Engineering, University of Aberdeen, Aberdeen, AB24 3UE, UK. Email: y.guo@abdn.ac.uk.

endanger the foundation and abutment of a dam. The erosion of plunge pool is closely related to the hydraulic energy dissipation in the plunge pool. There are many energy dissipation means. For example, the high velocity water jet from a slot in a dam or from a flip bucket and the waterfall over the spillway is among them. These energy dissipation means have many advantages, such as economy, simple engineering structure and a wide suitability for both the discharge and water depth downstream. Therefore, these energy dissipation means have been widely used in the medium and high dams. However they also present a challenge task to their designers. As highly turbulent water jet travels through atmosphere, it entrains air into it and becomes a mixture of air-water prior to impinging into plunge pool downstream. Studies showed that only 10-20 percent jet energy is dissipated during the trajectory process through the atmosphere (Elevatorski 1959); most jet energy is dissipated within plunge pool. Therefore, understanding of the mechanism of energy dissipation within plunge pool can improve the prediction of the erosion and scour. As free water jet becomes an air-water two-phase flow prior to entering pool, it is important to accurately estimate the effect of air entrained into the jet on the energy dissipation in plunge pool. Such energy dissipation is closely related to the spreading of the jet in plunge pool. This is the motivation of this study in which we aim to advance our knowledge and understanding of the effect of air content on the spreading of a jet in plunge pool.

Due to its practical importance, many laboratory experiments have been conducted to investigate the scour depth in plunge pool during the past decades. Several empirical formulas for predicting plunge pool scour depth have been proposed based on both the laboratory experiments and some prototype data (see, for example, Martins 1975; Rajaratnam and Beltaos 1977; Mason 1984; Mason and Arumugam 1985; Bormann and Julien 1991; Hoffmans 1998). The calculated results from these formulas, however, are different from each other (Mason and Arumugam, 1985). Such difference may be ascribed to the fact that most formulas only considered the effect of jet fall height and discharge per unit width, the characteristic size of bed materials, takeoff jet angle and tailwater depth on the scour depth, but did not take the influence of air content into account when evaluating the scour depth. In practical situation, turbulent free water jet becomes a two-phase flow (air-water mixture) prior to entering into water downstream as it entrains considerable air into it during its trajectory (Ervine *et al.* 1980). The study of Mason (1989a, b) indicated that the air entrained by turbulent free water jet should be taken as an additional parameter in the estimation of plunge pool scour. His study showed that the air content increased scour depth. However, his formula over-estimated scour depth when it was applied to the prototype data. The effect of air content on the scour depth has also been recently investigated by Bollaert and Schleiss (2003b); Canepa and Hager (2003); Xu *et al.* (2004) and Pagliara *et al*. (2006, 2008). The study of Xu *et al.* (2004) shows that for a rectangular jet, when both the water flow rate and air-water mixture jet velocity for aerated jet are the same as those of non-aerated jet, the scour depth is decreased with the increasing of air content. In their comparison, to keep the same water flow rate and jet velocity, aerated jet width is obviously larger than that of non-aerated jet. Canepa and Hager (2003) also indicated that caution should be taken which velocity – air-water mixtures or pure water – is used when evaluating the effect of air content on scour depth. For rectangular jets, which are typical of spillway discharge (Puertas and Dolz 2005), the formula presented by Ervine (1976) shows that the amount of air entrained by free jet with high velocity and large fall height is very large. More studies on plunge pool scour by a trajectory jet can be found in recent review papers by Hager (2007) and Bollaert and Schleiss (2003a).

Comparing with extensive laboratory experimental studies, relatively few numerical investigations have been conducted to evaluate the scour generated by free-falling jet. Jia *et al.* (2001) investigated the scouring process in plunge pool using CCHE3D model. Salehi Neyshabouri *et al.* (2003) carried out the similar study using a two-dimensional (2D) numerical model. Both studies did not examine the effect of jet air content on scour. As indicated by Jia *et al.* (2001), the pressure fluctuation, which is closely related to the velocity field, plays an important role in plunge pool scour. Therefore, this study is to examine the effect of jet air content on plunge pool scour using numerical simulations. We will focus on simulating the velocity and pressure field and spreading of aerated and non-aerated jets. To this end, a multiphase model is employed and described as following.

Multiphase model

The multiphase model embedded in FLUENT (ANSYS 12.0, 2009) is applied to simulate the effect of air content on the spreading of the falling water jet in plunge pool. Volume of fluid (VOF) is used in the simulation. In VOF models, water (primary phase) and air (secondary phase) share the same velocity and pressure field, therefore, a single set of momentum and continuity equations in conservative form is used to describe the flow. For convenience, a brief description is given as following.

Governing equations

The governing equations solved for each phase in the multiphase model can be written in a Cartesian coordinate system (shown as in Figure 1) as following:

Continuity equation:

$$\frac{\partial \rho}{\partial t} + \frac{\partial \rho u_i}{\partial x_i} = 0 \tag{1}$$

Momentum equation:

$$\frac{\partial \rho u_i}{\partial t} + \frac{\partial}{\partial x_j}(\rho u_i u_j) = -\frac{\partial p}{\partial x_i} + \frac{\partial}{\partial x_i}\left[(\mu + \mu_t)\bullet\left(\frac{\partial u_i}{\partial x_j} + \frac{\partial u_j}{\partial x_i}\right)\right] \tag{2}$$

k-equation:

$$\frac{\partial}{\partial t}(\rho k) + \frac{\partial}{\partial x_i}(\rho k u_i) = \frac{\partial}{\partial x_j}\left[\left(\mu + \frac{\mu_t}{\sigma_k}\right)\frac{\partial k}{\partial x_j}\right] + G_k + G_b - \rho\varepsilon \tag{3}$$

ε-equation:

$$\frac{\partial}{\partial t}(\rho\varepsilon) + \frac{\partial}{\partial x_i}(\rho\varepsilon u_i) = \frac{\partial}{\partial x_j}\left[\left(\mu + \frac{\mu_t}{\sigma_\varepsilon}\right)\frac{\partial \varepsilon}{\partial x_j}\right] + C_{1\varepsilon}\frac{\varepsilon}{k}(G_k + C_{3\varepsilon}G_b) - C_{2\varepsilon}\rho\frac{\varepsilon^2}{k} \tag{4}$$

where ρ, μ =density and dynamic viscosity of air-water mixture, respectively; t = time; u_i = component of velocity in the x_i-direction; p = pressure; k = turbulent kinetic energy (TKE), ε = rate of dissipation of TKE, μ_t = turbulent (or eddy) viscosity, σ_k, σ_ε = turbulent Prandtl number for k and ε, respectively; G_k = TKE produced by the mean velocity gradients, G_b = TKE produced by buoyancy.

The turbulent viscosity can be determined using the turbulent kinetic energy (k) and its dissipation rate (ε):

$$\mu_t = \rho C_\mu \frac{k^2}{\varepsilon} \tag{5}$$

The values of the constants in above equations are (Rodi 1993): σ_k =1.0; σ_ε =1.3; C_μ=0.09; $C_{1\varepsilon}$=1.44; and $C_{2\varepsilon}$=1.92.

The term of turbulent kinetic energy produced by the mean velocity gradients G_k can be determined by

$$G_k = \mu_t \left(\frac{\partial u_i}{\partial x_j} + \frac{\partial u_j}{\partial x_i} \right) \frac{\partial u_i}{\partial x_j} \tag{6}$$

The density and viscosity of air-water mixture is a function of the volume fraction and can be determined as (ANSYS 12.0, 2009):

$$\rho = (1-\beta_0)\rho_w + \beta_0 \rho_a \tag{7}$$

$$\mu = (1-\beta_0)\mu_w + \beta_0 \mu_a \tag{8}$$

where β_0 = volumetric fraction of air; ρ_w, ρ_a = density of water and air, respectively; μ_w, μ_a = viscosity of water and air, respectively.

Numerical scheme

Figure 1 shows the computational domain. To improve the calculation accuracy and reduce the computational time, the unstructured non-uniform triangular meshes are used in the computational domain. This allows the locally refining the concerned regions (e.g. near the jet core and the region near the tank bottom) with small meshes and has advantage of flexibly assigning meshes in the computational domain (Guo et al. 2008, 2012). The sensitivity of mesh size was investigated by adapting and refining the meshes until no significant changes in the solution were achieved. Meanwhile, the effect of meshes on the convergence of numerical simulations was also examined. The final meshes used in the simulation had 43275 (for shallow water) ~58277 (for deep water) nodes and 85248 (for shallow water) ~ 115200 (for deep water) cells, with the minimum 0.002m grid size near the jet core and tank bottom and the maximum 0.004m grid size in other regions. The second order implicit method is applied for temporal discretization, while highly stable power-law differencing is used for spatial discretization of governing equations. The phase coupled SIMPLE (PC-SIMPLE) is applied for pressure-velocity coupling (Vasquez and Ivanov 2000). To speed up the convergence of simulation, the under-relaxation technique was used by changing the under-relaxation factor during the calculation. This was done carefully so that no divergence or undue instability occurred (Guo *et al*. 2007).

Boundary conditions

At the inlet boundary, average velocity and jet slot width are specified according to the laboratory experiments (Guo and Luo 1999). Turbulent kinetic energy (k) and its dissipation rate (ε) at the inlet boundary are calculated as (Jing *et al*. 2009):

$$k = 1.5(IU_0)^2 \tag{9}$$

$$\varepsilon = c_\mu^{3/4} \frac{k^{3/2}}{l} \tag{10}$$

where I = turbulent intensity and taken as 10% in this study; U_0= average velocity at the inlet (see Figure 1); l (= 0.07 R) = turbulence length scale, and R = the hydraulic radius at the inlet and taken as the jet slot width d. For aerated jet, the initially prescribed air content, thus the flow rate weighting, is specified at the inlet while the tank is filled with pure water. At the free water surface, the atmospheric pressure is applied and adjusted according to the air-water flow rate weighting in the simulation. At the two outlets (see Figure 1), the pressure outlet boundary condition is specified in which a static pressure at the outlet boundary is realized. . On all solid boundaries, including side walls and the bottom of tank, no-slip boundary condition is applied.

Model validation

The multiphase model is validated using the laboratory experiments of Guo and Luo (1999). Though the experimental details can be found in Guo and Luo (1999), we present a brief description for convenience and completeness. The experiments were conducted in a tank of 34 cm wide and 180 cm long with changeable water depth. Two water depths of 29 cm and 39 cm were used in the experiments while several water depths were investigated in numerical simulations. Jet velocity at exit was maintained as constant throughout the experiments by constant water head. For aerated jet, air with prescribed flow rate was fed into pressure relief chambers and a box with small holes upstream by an air compressor. Therefore, air had moved a distance and uniformly mixed with jet water prior to entering into tank. To avoid extra air entrained by jet into tank at the water surface, jet was introduced immediately below the water surface so that the influence of air content could be effectively evaluated. The hydrodynamic pressure at tank bottom was measured using Multi-point Pressure Scanner manufactured by Scanivalve of USA with the accuracy of ±0.5% and pressure range of 0.007 m to 10 m (water height). The Scanner was linked with 23 manometer tubes with the inner diameter of 1 mm. The distances between two tubes varied from 5mm to 20mm. The experimental parameters were: air content (defined as the ratio of air volume to air-water volume) was β_0 =27% ~ 44%; the mean jet velocity U_0 at exit was from 3.4 m/s to 5.7 m/s; the slot width of the pure water jet (d) was 1.0 cm, 1.6 cm, 2 cm, 2.5 cm, 3 cm, 4 cm and 5 cm, respectively. For aerated jet, the equivalent water width at exit is the total width of the air-water mixture times (1- β_0). The corresponding Reynolds number (defined as $Re=U_0d/\nu$,) was from 54400 to 285000 so that jet was completely turbulent flow (Fischer *et al*. 1979).

Results and discussions

Spreading of jet

The spreading of a jet determines the extent of scour hole caused by jet. The spreading of a jet can be evaluated by the angle of jet spreading and the velocity profile at a distance from jet exit. Two jet spreading scales are used and investigated. The first is the half jet width at which velocity drops to the half of the jet centreline velocity while another scale is the jet spreading angel determined using the jet boundary whose velocity is 5% of the jet centreline velocity at the same distance from exit. For pure water jet, the simulated averaged half jet width over the distance being greater than 6 times of jet width at exit is about 0.102 of that distance. This value agrees well with the experimental measurements of Kuang *et al.* (2001) (0.1~0.12) and Miozzi *et al.* (2010) (~0.10) for turbulent plane jet. This spreading value is also reasonably compared with other published data for turbulent plane jets (Fischer *et al.* 1979; Chu and Lee 1999). The simulated averaged jet spreading angle determined using 5% of centreline velocity for pure water jet is about 9.2 ±1 degree, which is slightly smaller than the value of laboratory measurements (10~11 degree) (Ervine and Falvey 1987). For aerated jet, the simulated averaged jet spreading angle is 12.9±1 degree, which is in good agreement with the measured value 13~14 degree of Ervine and Falvey (1987).

Simulations were also run for a range of jet slot width, Reynolds number, tank water depth and air content to examine their effects on jet spreading. The results indicate that no significant effect of such parameters on the spreading of jet.

Velocity profile

It is well known that the velocity profile at the jet cross section being more than six times of jet diameter downstream has a self similar form and Gaussian distribution for a pure water jet (Fischer *et al.* 1979). For the problem under investigation, the water depth in tank is relatively shallow and jet diffusion in water is restricted. Vortices are generated near the tank bottom at both sides of jet, affecting velocity field. For aerated jet, air content may also play a role in jet velocity profile. To examine if the velocity profile for aerated jet fits a Gaussian distribution, numerical simulations have been performed covering a range of jet Reynolds numbers, air contents at exit and water depths in tank. Figure 2 is a typical example of the simulated and measured velocity profiles for aerated jet: β_0=27%, *Re*=58,400, *H/d*=26.7, In Figure 2, velocity is normalized using the local centreline (maximum) velocity while horizontal distance is normalized by local vertical distance from exit. To examine the self –similar Gaussian distribution, simulated velocity profiles at three downstream distances (*z/d*=3.7; 6.5 and 16) are plotted in Figure 2. It is seen that when jet is in the near region from slot (*z/d*=3.7); normalized velocity distribution shows a top hat velocity profile, demonstrating that jet is still in the zone of flow establishment (Fischer *et al.* 1979). The velocity profiles at the downstream distance being larger than six slot width, however, demonstrate perfect self –similar Gaussian distribution. Numerical runs performed for various air contents (up to 50%), Reynolds numbers and tank water depths reveal similar results to Figure 2, indicating that air content has little effect on the self-similarity of jet velocity profile for the flow conditions simulated. In all numerical simulations performed no air bubbles within jet move upwards and escape from tank as their downward velocity is larger than the critical velocity of 0.26m/s (Mckeogh and Ervine 1980). Good agreement between the measured and simulated velocity profiles demonstrates that the model is capable to calculate the spreading of aerated jet in a tank with finite water depth.

Numerical simulations carried out for non-aerated jet for a range of Reynolds numbers and tank water depths also reveal similar results. Figure 3 is a typical example of the simulated velocity profile at various water depths for Re=80,000 and water depth in tank H=39 cm (H/d=19.5). The solid line is the averaged velocity profiles at four positions whose downstream distance (z/d) is greater than 5 slot widths and smaller than 15 slot widths. The results show that the self-similar Gaussian profile is valid for z/d being greater than 5. A top hat velocity profile is also found for $z/d<4$ where flow is in the zone of flow establishment. When velocity profile is taken at z/d=17, which is close to the tank bottom (at tank bottom z/d= H/d =19.5), the boundary edge of jet is influenced by the vortices formed there. In general, the numerically simulated velocity profile is in good agreement with the experimental measurements.

Velocity decay

Local maximum velocity, usually occurring at the jet centreline, is a key parameter which primarily determines the plunge pool scour depth. As jet water flows downstream, jet expends due to the ambient water entrained into it and its velocity decreases. It is of engineering importance to investigate how the jet parameters influence the decay of the jet centreline velocity. Figure 4 shows the variation of the simulated and measured centreline jet velocity U_m normalized by the velocity at exit U_0 with the dimensionless distance from the jet exit. Some experimental data by other investigators are also plotted in Figure 4 for comparison. For aerated jet, the jet width used in the figure is the equivalent pure water width. It is seen that the simulated jet centreline velocity decay with downstream distance from exit agrees well with the laboratory experiments of Guo and Luo (1999). This may not be surprised as the flow parameters and geometry used in the numerical model are identical to those in experiments. The results also show that the air content has insignificant effect on the jet centreline velocity decay.

Comparison of this numerical simulation with the experimental results of Miozzi *et al.* (2010) and Kuang *et al.* (2001) reveals that relatively large discrepancy between measurements and simulation exists. In both comparison cases, the numerical model underestimates the decay of centreline velocity with downstream distance. In particular, experiments by Kuang *et al*. (2001) shows a rapid decay of the centreline velocity with distance while numerical simulation demonstrates gradual decrease of the centreline velocity. This discrepancy between numerical simulation and experiments may be ascribed to the different boundary conditions as well as different geometry (Kim and Choi 2009). When jet is bounded in all directions (the situation of the present work), a slower decrease of velocity is expected (Miozzi *et al*. 2010).

Though there exists relatively large deviation between the numerical simulation and the experimental measurements of Kuang *et al*. (2001), the slope of the centreline velocity decay with distance is similar. This can be revealed by expressing the variation of the jet centreline velocity with downstream distance for a plane turbulent jet as:

$$\frac{U_m}{U_0} = k(\frac{d}{z})^{1/2} \qquad (11)$$

where coefficient k determines the speed of the jet centreline velocity decay. The value of k reported by Guo and Luo (1999) is 2.75 for nonaerated jet and 2.87 for aerated jet. For a pure water jet, Beltaos (1976) had a value of 2.72; Davies *et al.* (1975) obtained a value of 2.62; Fischer *et al*. gave a value of 2.41 while Gutmark and Wygnanski's experiments (1976) showed a value of 2.4. The recent study of Miozzi *et al.* (2010) found a value of 2.35. The present numerical study shows that the value is 2.58 for non-aerated jet and 2.62 for aerated jet; which agrees well with that reported by Davies *et al*. (1975); but is smaller than those of Belatos (1976) and Guo and Luo (1999) and slightly greater than others.

Maximum pressure at tank bottom

The maximum pressure at the tank bottom is another key parameter determining plunge pool scour hole depth. Figure 5 shows the variation of the maximum pressure at the tank bottom with the flow Reynolds number for tank water depth of 29 cm (5a) and 39 cm (5b). For aerated jet, two velocities are used to calculate the Reynolds number, namely the water velocity U_0 and air-water mixture velocity $U_{aw}=U_0/(1-\beta_0)$ (Canepa and Hager 2003). In both cases, the equivalent slot water width is used in calculating the Reynolds number. This means that for the same U_0 and width of air-water mixture, the Reynolds number will decrease with increase of air content. Experimental results of Guo and Luo (1999) for nonaerated jet are also plotted for comparison. The data is a bit scatter. In general, the maximum pressure at the tank bottom increases with the increase of the flow Reynolds number for both the aerated and non-aerated jet. The simulation is reasonably compared with the experimental measurements of Guo and Luo (1999). Figure 5 demonstrates that when only pure water jet velocity is used in aerated jet, the maximum pressure for aerated jet is larger than that of nonaerated jet for the same Reynolds number. This is because the equivalent slot water width for aerated jet is smaller than that of nonaerated jet, thus leading to the decrease of the Reynolds number. Numerical runs also reveal that the maximum pressure increases with the increase of air content provided that the water flow rate and the slot width remains unchanged. In this situation the added air will increase jet velocity from U_0 to $U_0/(1-\beta_0)$. However, when the aerated jet velocity is the same as the pure water jet velocity, the maximum pressure of aerated jet is smaller than that of nonaerated jet due to the decrease of the density of aerated jet. This conclusion is consistent with that of Canepa and Hager (2003).

Effect of air content on pressure distribution at the tank bottom

Figure 6 shows the effect of air content on the pressure distribution at the tank bottom for jet slot width of 1.6 cm, U_0 =3.4m/s and β=0, 27%, 36% and 44%, respectively. In numerical simulation, jet velocity and jet slot width at exit remains unchanged. As such, the increase of air content means the decrease of water fraction in jet, namely the jet density decreases. This causes the decrease of pressure, as shown in Figure 6. Numerical runs were performed for a range of jet velocity and width at exit, water depth in tank and air content at exit, obtaining the similar results shown as in Figure 6.

Conclusion

Numerical simulations are performed to investigate the spreading of aerated and nonaerated jet in a tank with finite water depth. Simulations cover a range of jet parameters, such as jet velocity and jet slot width at exit, initial air content at exit and water depth in tank. The results show that the self-similar Gaussian distribution of jet cross sectional velocity profiles exists for the downstream distance which is larger than five jet slot width for both aerated and nonaerated jets. Air content has little influence on velocity profile. The decay of the jet centreline velocity with downstream distance is simulated for a range of flow conditions. Good agreement between the simulation and laboratory measurements with the identical flow conditions and geometry is obtained. Comparison of the numerical simulation with the experimental results of Miozzi *et al.* (2010) and Kuang *et al.* (2001) reveals that the numerical model underestimates the jet centreline velocity decay. This discrepancy between numerical simulation and experiments may be ascribed to the different boundary conditions and geometry (Kim and Choi 2009). In present study, the jet is bounded in all directions, thus, slower velocity decay is expected (Miozzi *et al*. 2010).

The effect of air content on pressure distribution and the maximum pressure at the tank bottom is simulated for various flow conditions. Caution needs to be taken for choosing jet velocity when evaluating the effect of air content on pressure. When the aerated jet velocity and width at exit remains unchanged, increasing air content means the decrease of water fraction in aerated jet. Consequently, density of aerated jet decreases, leading to the decrease of pressure. In practical situation, when air is entrained into jet, jet cross section and the total air-water flow rate will increase. Consequently, the scour hole downstream will become larger, shallower and flatter (Mason 1989a, b).

Acknowledgements: This work is partly supported by the Open Funding from the State Key Laboratory of Hydraulics and Mountain River Engineering, Sichuan University (SKHL1302). The author is grateful for Mairi Ng and Megan Johnston who conducted some simulation work as part of their MEng projects at University of Aberdeen. The constructive comments made by three anonymous reviewers have significantly improved the quality of the paper.

References

ANSYS FLUENT (2009). “Theory Guide and User’s Guide, version 12.0.” *ANSYS, Inc.* Southpointe, Canonsburg, U.S.

Beltaos, S. (1976). “Oblique impingement of plane turbulent jets.” *J. Hydr. Div.*,102(9), 1177-1192.

Bollaert, E. and Schleiss, A. (2003a). “Scour of rock due to the impact of plunging high velocity jets Part I: a state-of-art review.” *J. Hydraul. Res.*, 41(4),451-464.

Bollaert, E. and Schleiss, A. (2003b). “Scour of rock due to the impact of plunging high velocity jets Part II: experimental results of dynamic pressures at pool bottoms and in one- and two-dimensional closed end rock joints.” *J. Hydraul. Res.*, 41(4), 465-480.

Bormann, E. and Julien, P.Y. (1991). “Scour downstream of grade-control structures.” *J. Hydraul. Eng.*, 117(5), 579-594.

Canepa, S., and Hager, W.H., (2003). “Effect of jet air content on plunge pool scour.” *J. Hydraul. Eng.*, 129: 358-365.

Chu, P.C.K. and Lee, J.H.W. (1999). An inclined wall jet: mean flow characteristics and effects of acoustic excitation. *J. Hydraul. Eng.*, 125, 193-205.

Davies, A.E., Keffer, J.F. and Baines, W.D. (1975). “Spread of a heated plane turbulent jet.” *Physics of Fluids*, 18(7), 770-775.

Elevatorski, E.A., (1959). Hydraulic energy dissipaters, McGraw-Hill, Ervine,D.A. (1976). “The entrainment of air in water.” *Int. Water Power and Dam Constr.*, 28, 27-30.

Ervine,D.A., McKeogh, E and Elsawy, E.M., (1980). “Effect of turbulence intensity on the rate of air entrainment by plunging water jet”, *Proc., Inst. Civ. Engrs., Part 2- Research and Theory*, 69, 425-445.

Ervine, D.A. and Falvey, H.T., (1987). “Behaviour of turbulent water jets in the atmosphere and in plunge pools.” *Proc., Inst. Civ. Engrs., Part 2- Research and Theory*, 83, 295-314.

Fischer, H.B., et al., (1979), Mixing in Inland and Coastal Waters, New York, Academic Press.

Guo, Y.K. and Luo, M. (1999). “Experimental study on the effects of air entrainment on a plane jet diffusion in a plunge pool.” *J. Hydrodynamics*, 11(2), 32-37.

Guo, Y.K., Wang, P. and Zhou, H. (2007). “Modelling study of the flow past irregularities in a pressure conduit.” *J. Hydraul. Eng.*, 133(6), 698-702.

Guo, Y.K., Zhang, L.X., Shen, Y.M. and Zhang, J.S., 2008. Modelling study of free overfall in a rectangle channel with strip roughness, *J. Hydraul. Eng.*, 134(5), 664-668.

Guo, Y.K., Wu, X.G., Pan, C.H. and Zhang, J. (2012). “Numerical simulation of the tidal flow and suspended sediment transport in the Qiantang Estuary.” *Journal of Waterway, Port, Coastal and Ocean Engineering*, 138: 192-203.

Gutmark, E. and Wygnanski, J. (1976). “The planar turbulent jet.” *J. Fluid Mech.*, 73, 465-495.

Hager, W.H., (2007). “Scour in hydraulic engineering.” *ICE Water Management*, 160:159-168.

Hoffmans, G.J.C.M. (1998). “Jet scour in equilibrium phase.” *J. Hydraul. Eng.*, 124(4), 430-437.

Jia, Y.F., Kitamura, T., and Wang, S.S.Y., (2001). “Simulation of scour process in plunging pool of loose bed-material.” *J. Hydraul. Eng.*, 127, 219-229.

Jing, H, Guo, Y.K., Li, C and Zhang, J., (2009). “Three-dimensional numerical simulation of compound meandering open channel flow by Reynolds stress model.” *International Journal for Numerical Methods in Fluids,* 59:927-943.

Kim, J. and Choi, H. (2009). “Large eddy simulation of a circular jet: effect of inflow conditions on the near field.” *J Fluid Mech.* 620: 383-411.

Kuang, J., Hsu, C.T. and Qiu, H. (2001). “Experiments on vertical turbulent plane jets in water of finite depth.” *J. Eng. Mech.* 127(1), 18-25.

Martins, R.B.F. (1975). “Scouring of rocky riverbeds by free-jet spillways.” *Water Power Dam Constr.,* 27(4), 152-153.

Mason, P.J. (1984) “Erosion of plunge pools downstream of dams due to the action of free-trajectory jets.” *Proc., Inst. Civ. Eng.*, Part 1, 76, 523-537.

Mason, P.J. and Arumugam, K. (1985) “Free jet scour below dams and flip buckets.” *J. Hydraul. Eng.*, 111, 220-235.

Mason,P.J., (1989a) “Effects of air entrainment on plunge pool scour.” *J. Hydraul. Eng.*, 115, 385-399.

Mason,P.J., (1989b) “Discussion of ‘Effects of air entrainment on plunge pool scour.’” *J. Hydraul. Eng.*, 115, 385-399.

McKeogh, E.J. and Elsawy, E.M. 1980. “Air entrained in pool by plunging water jet.” *J. Hydr. Div., ASCE*, 106: 1577-1593.

Miozzi, M., Lalli, F. and Romano, G.P. (2010). “Experimental investigation of a free-surface turbulent jet with Coanda effect.” *Exp. Fluids,* 49, 341-353.

Pagliara, S., Hager, W.H., and Minor, H.E. (2006). “Hydraulics of plane plunge pool scour.” *J. Hydraul. Eng.*, 132(5), 450-461.

Pagliara, S., Massimiliano, A. and Hager, W.H. (2008). “Hydraulics of 3D plunge pool scour” *J. Hydraul. Eng.*, 134(9), 1275-1284.

Puertas, J. and Dolz, J. (2005). “Plunge pool pressure due to a falling rectangular jet.” *J. Hydraul. Eng.*, 131(5), 404-407.

Rajaratnam, N. and Beltaos, S. (1977) “Erosion by impinging circular turbulent jets.” *J. Hydr. Div.*,103(10), 1191-1205.

Rodi, W. (1993). *Turbulence models and their application in hydraulics: a state-of-the-art review*. 3rd edition, A.A.Balkema, Rotterdam, Netherlands.

Salehi Neyshabouri, A.A., Ferreira Da Silva, A.M., and Barron, R.(2003). “Numerical simulation of scour by a free falling jet.” *J. Hydraul. Res.*, 41, 533-539.

Vasquez, S.A., and Ivanov, V.A. (2000). “A phase coupled method for solving multiphase problems on unstructured meshes.” *Proc. ASME FEDSM’00: ASME 2000 Fluids Engineering Division Summer Meeting*, ASME, New York.

Xu, W., Deng, J., Qu, J., Liu, S. and Wang, W. (2004). “Experimental investigation on influence of aeration on plane jet scour.” *J. Hydraul. Eng.*,130(2), 160-164.

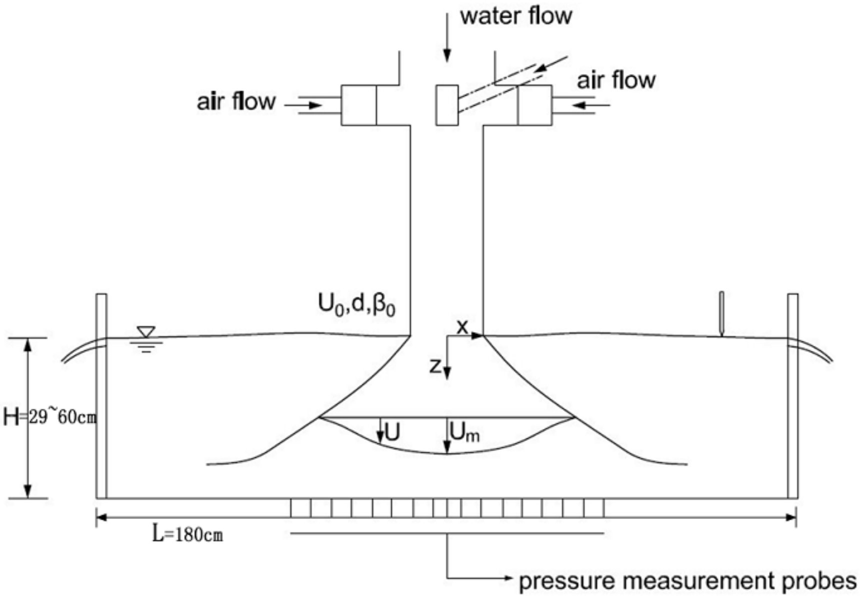

Figure 1. The sketch of the computational domain and experimental set-up of Guo and Luo (1999).

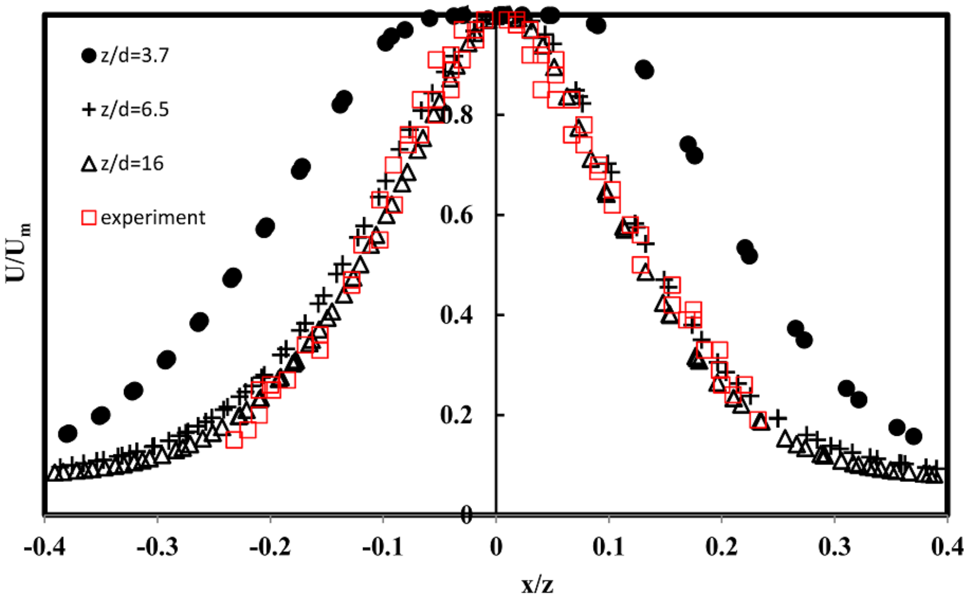

Figure 2. Comparison of simulated and measured velocity profiles for aerated jet at various distances downstream from exit: β0=27%, Re=58,400, H/d=26.7. Velocity is normalized by the local centreline velocity while horizontal distance is normalized by vertical distance from exit.

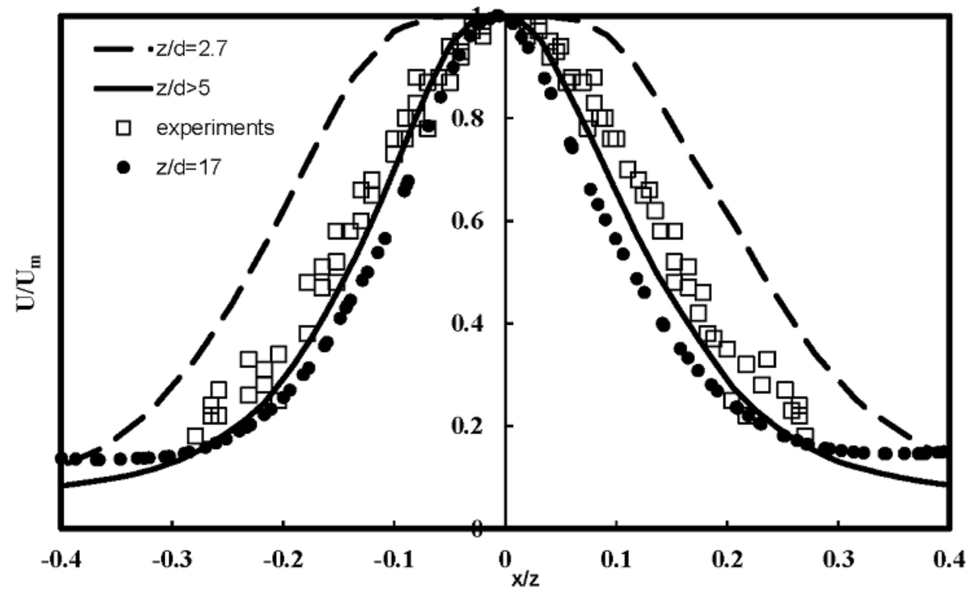

Figure 3. Comparison of simulated and measured velocity profiles for nonaerated jet at various distances from exit: Re=80,000 and H/d=19.5. Velocity and horizontal distance are normalized in the same way as in Figure 2.

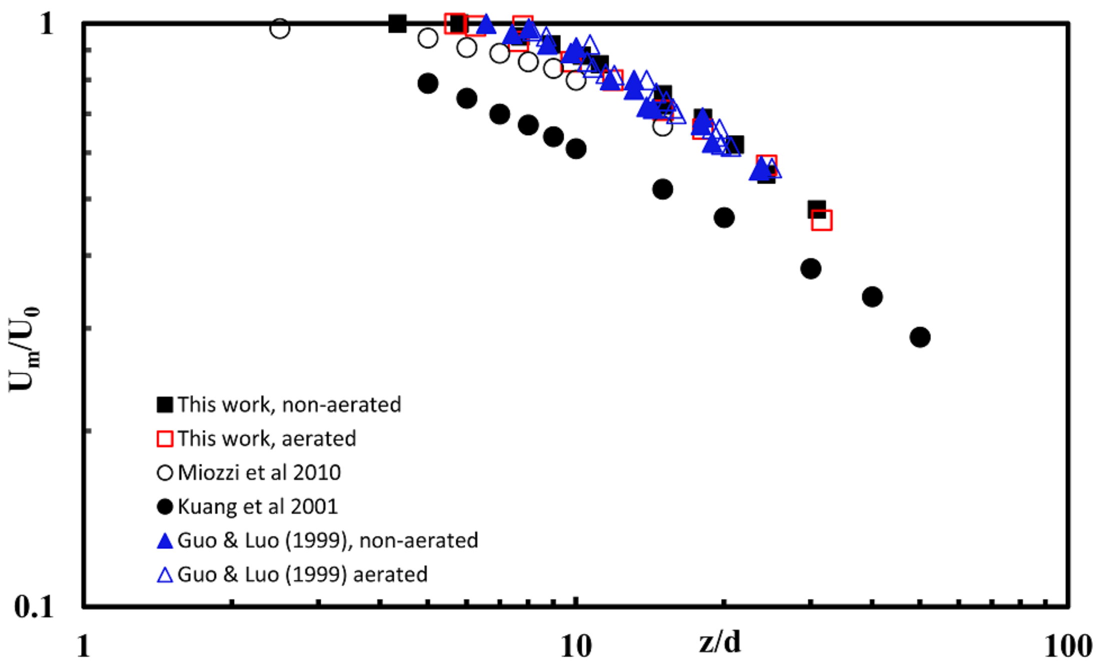

Figure 4. Variation of normalised jet centreline velocity decay with distance downstream from exit for various flow conditions. Experiments by Guo and

Luo(1999), Kuang et al. (2001) and Miozzi et al. (2010) are included for comparison.

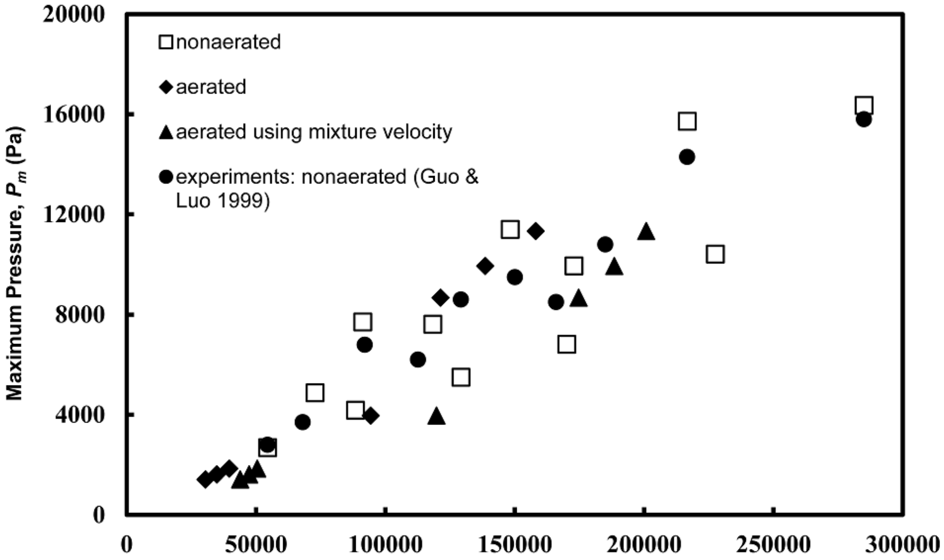

Figure 5(a)

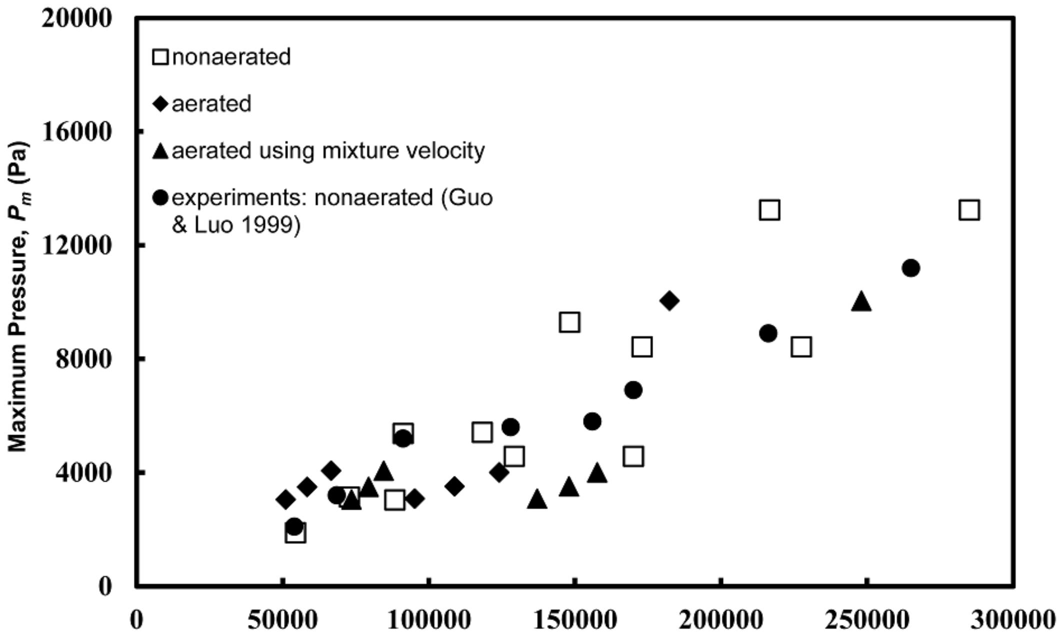

Figure 5(b)

Figure 5. The maximum pressure at the tank bottom for both aerated and nonaerated jets for various flow conditions, (a) water depth at tank H=29 cm; (b) H=39 cm

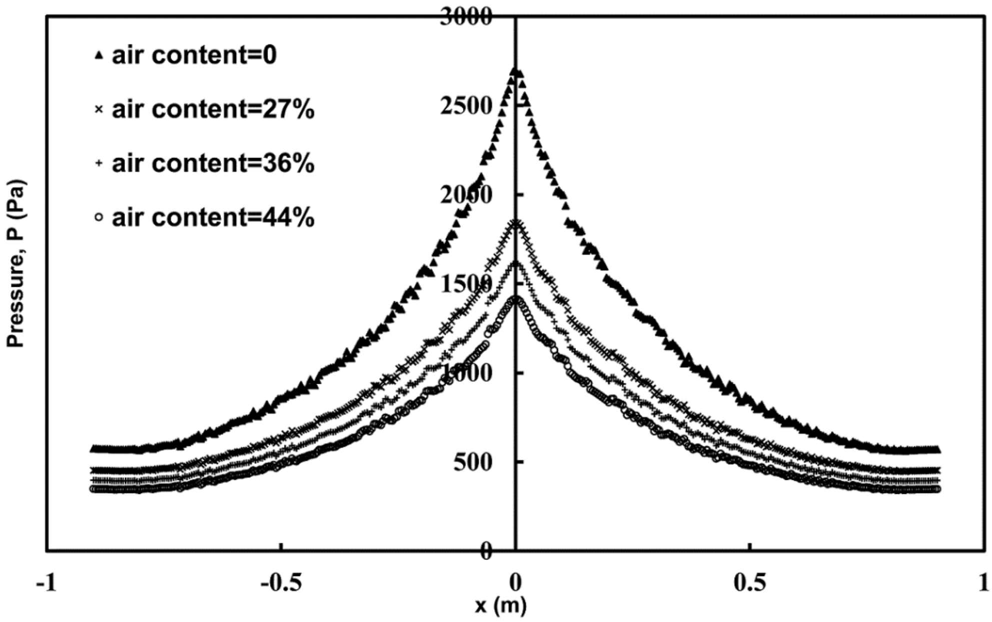

Figure 6. Effect of air content on pressure distribution at tank bottom for d=1.6 cm, U0 =3.4m/s, H=29 cm and β=0, 27%, 36% and 44%, respectively.